ELSEVIER

Catalysis Today 83 (2003) 141–156

CATALYSIS TODAY

www.elsevier.com/locate/cattod

Transient modeling of combined catalytic combustion/CH_4 steam reforming

Fletcher A. Robbins, Huayang Zhu[1], Gregory S. Jackson*

Department of Mechanical Engineering, University of Maryland, College Park, MD, 20742 USA

Received 1 May 2002; received in revised form 3 March 2003; accepted 18 March 2003

Abstract

This paper presents an investigation into the complex interactions between catalytic combustion and CH_4 steam reforming in a co-flow heat exchanger where the surface combustion drives the endothermic steam reforming on opposite sides of separating plates in alternating channel flows. To this end, a simplified transient model was established to assess the stability of a system combining H_2 or CH_4 combustion over a supported Pd catalyst and CH_4 steam reforming over a supported Rh catalyst. The model uses previously reported detailed surface chemistry mechanisms, and results compared favorably with experiments using a flat-plate reactor with simultaneous H_2 combustion over a γ-Al_2O_3-supported Pd catalyst and CH_4 steam reforming over a γ-Al_2O_3-supported Rh catalyst. Results indicate that stable reactor operation is achievable at relatively low inlet temperatures (400 °C) with H_2 combustion. Model results for a reactor with CH_4 combustion indicated that stable reactor operation with reforming fuel conversion to H_2 requires higher inlet temperatures. The results indicate that slow transient decay of conversion, on the order of minutes, can arise due to loss of combustion activity from high-temperature reduction of the Pd catalyst near the reactor entrance. However, model results also show that under preferred conditions, the endothermic reforming can be sustained with adequate conversion to maintain combustion catalyst temperatures within the range where activity is high. A parametric study of combustion inlet stoichiometry, temperature, and velocity reveals that higher combustion fuel/air ratios are preferred with lower inlet temperatures ($\leq$500 °C) while lower fuel/air ratios are necessary at higher inlet temperatures (600 °C).

Keywords: Catalysis; Combustion; Steam reforming; Palladium; Rhodium; Methane; Hydrogen; Reactor modeling

1. Introduction

The development of volumetrically efficient reactors for production of H_2 from hydrocarbons for fuel cell applications [1–3] or for H_2 addition to improve stability of lean-premixed combustion systems [4,5] presents new challenges to reactor designers. Development of compact steam reformers or partial oxidation systems with high fuel conversion, consistent H_2 selectivity, and minimal pressure drop will greatly benefit from improved modeling capable of assessing these performance criteria in both catalytic as well as non-catalytic systems. More advanced modeling tools including detailed surface kinetics can greatly expand the ability to evaluate critical design tradeoffs for optimizing H_2 production reactors.

With simplified models, researchers have shown that maximum heat transfer rates to the reforming

* Corresponding author. Tel.: +1-301-405-2368; fax: +1-301-314-9477.
E-mail address: gsjackso@eng.umd.edu (G.S. Jackson).
[1] Present address: Engineering Division, Colorado School of Mines, Golden, CO 80401, USA.

0920-5861/$ – see front matter © 2003 Elsevier B.V. All rights reserved.
doi:10.1016/S0920-5861(03)00225-6

catalyst are necessary for optimizing reformer designs for compactness and fast response during start-up [6]. One approach that has been explored for providing extremely high heat transfer rates to reforming catalysts and thus high volumetrically efficiency for hydrocarbon to H_2 conversion involves a reactor with heat-exchanger-like flow paths where exothermic catalytic combustion provides heat across a flow separating surface to drive endothermic steam reforming. Such reactors have taken various geometric configurations including parallel plate catalytic reactors [7] or co-axial catalyst supports [8], where the combustion catalyst and reforming catalyst are separated by a non-porous (but relatively thin) structure. These steam reforming-based approaches to H_2 production stand in contrast to alternative partial oxidation reactors [1,2,9] and present some advantages over the self-sustaining partial oxidation reactors, particularly for situations where pure steam is readily available. Advantages of the combined catalytic combustor/steam reformer include higher exiting H_2 mole fractions in the "reformate" stream (which results in reduced over-potentials for fuel cell anodes) and also the potential to utilize otherwise lost fuel chemical energy, such as excess H_2 in the fuel cell anode exhaust, for the catalytic combustion fuel.

With an integrated catalytic combustion/steam reforming reactor, the combination of a large heat sink (steam reforming) and a large heat source (catalytic combustion) on opposite sides of the surface raises questions about the design and operability of such a reactor. These issues are particularly complicated with the use of Pd-based catalysts, which are the most active catalyst for CH_4 combustion. The tendency for Pd-based catalysts to change oxidation states and thus activity at high temperature under flow conditions can compromise reactor performance because of catalyst deactivation or in some cases, potential surface temperature runaway [10–12]. This combined with the need for high temperatures in steam reforming catalysts to provide adequate CH_4 conversion and to avoid surface carbon build-up [13] places limitations on the operating window of a combined catalytic combustor/steam reformer using CH_4 as the reforming fuel. The current study explores some issues for H_2 production from natural gas by employing a model of a simplified reactor configuration of parallel flat plates with alternative passages for CH_4 steam reforming and H_2 or CH_4 catalytic combustion. This configuration is simulated with a transient flow model using multi-step surface chemistry to explore reactor operability and stability for a range of operating conditions. The modeling study can also be used to explore reactor design for optimal H_2 production.

Fig. 1 shows a schematic of the reactor configuration used in the current study. A thin flat plate with supported washcoat coatings on opposite sides separates the catalytic combustion channel from the reforming channel. The use of thin washcoat supports can provide the potential for very high heat fluxes (indicated in Fig. 1) since both the chemical heat generation and heat removal occur directly at the surface. Maximum heat fluxes q_{max} across this surface can be determined from the product of the heat of reforming

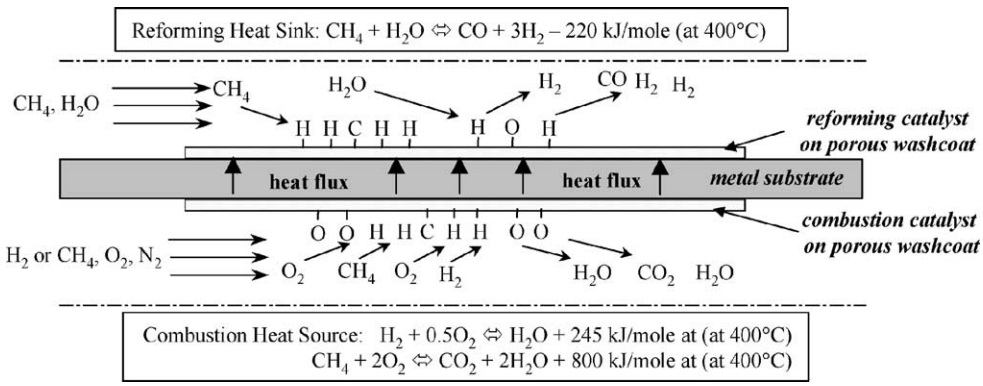

Fig. 1. Schematic diagram of integral catalytic combustion/steam reforming configuration modeled in this study. Dashed lines represent lines of symmetry in flow channels. Schematic is not to scale.

ΔH_{reac} times the mass transfer limit to the surface reaction on the reforming side. For CH_4 reforming, q_{max} can be approximated by

$$q_{max} = \left(\frac{P}{RT}\right)(Sh_{CH_4} D_{CH_4}) \frac{X_{CH_4}}{d_{chan}} \Delta H_{reac} \quad (1)$$

where $Sh_{CH_4} D_{CH_4}$ is the product of the Sherwood number and the effective diffusivity for CH_4 (assumed to be the limiting reactant), X_{CH_4} the mole fraction of CH_4 in the channel flow and d_{chan} the channel diameter. For cases similar to the current study with $T_{in} = 600\,^{\circ}C$, $P_{in} = 1$ bar, $V_{in,ref} \approx 6$ m/s and $d_{chan} \approx 1.0$ mm, q_{max} ranges from 6 to 8 W/cm^2, which is over 10 times larger than what standard convection heat transfer from gas-phase combustion products would provide if used to heat the surface indirectly. However, with these high heat fluxes, the integral combustor/reformer must maintain reactor surface temperatures within limits to avoid high temperature deactivation either for the combustor catalyst (in this study a supported Pd catalyst [12]), or the reforming catalyst (in this study, a supported Rh catalyst [14]).

The dynamic behavior of the integral combustor/steam reformer during start-up as well as during conditions where either the combustion or reforming catalyst is undergoing changes in activity must be understood to design a reliable reactor configuration. To that end, a transient model as described below using previously reported mechanisms for Pd-based catalytic combustion [15] and Rh-based reforming [16] was developed to investigate the transient behavior of the simplified reactor configuration presented in Fig. 1. Rhodium was chosen as the reforming catalyst because experiments revealed that more conventional nickel catalyst did not provide adequate activity at low temperatures to provide good conversion at temperatures below the deactivation temperatures of PdO_x combustion catalysts (between 700 and 800 °C at atmospheric pressure). For such a co-flow reforming and combustion system, reactor performance can vary widely depending on the relative flow velocities, combustion equivalence ratios, and reactor inlet temperatures. The model was validated by comparing predicted performance with that observed in experiments of a reactor of similar geometry. The current study focuses on the dynamic relationship between the catalytic combustion and the catalytic steam reforming of CH_4 during transient start-up when both catalysts can experience significant changes in activity before attaining steady state.

2. Model description

The numerical model in this study was adapted from previously reported single channel models [15,17] for investigating the transient behavior of catalytic combustors with washcoat-supported catalysts. The current model combines two single channel models with multi-step surface chemistry for each catalyst and a finite volume heat transfer model for the separating surface to predict the transient behavior of the integrated reforming and combustion processes. Because the time scales involved in the integrated reactor can be on the order of several minutes, the channel flow models needed to be reasonably fast such that transient integration could occur over such long time scales. To achieve this goal, a transient quasi-one-dimensional formulation was implemented for each channel flow where local heat and mass transfer correlations were used to determine the differences in temperatures and species concentrations between each channel flow and their respective porous washcoats. A brief discussion of the model features is provided here.

2.1. Gas-phase model

The channel flow model used transient one-dimensional flow equations with the possibility of allowing for gas-phase reactions. The governing equations for the gas-phase flow were simplified from the previously reported model [15] by assuming negligible axial diffusion of heat or mass in the gas phase and assuming isobaric conditions. These assumptions had a negligible impact on the species and temperature profiles, and the isobaric assumption allowed for larger time steps in the transient integration by avoiding limitations associated with the compressible flow equations. For heat and mass transport from the channel flow to the catalytic washcoat boundary, the model used modified Graetz number heat and mass transfer correlations for reacting laminar flow based on a previous study [18]. A discussion on how these correlations compare to assessments of heat and mass transfer to the catalyst in a full two-dimensional model are discussed elsewhere [15,19]. Although their range

of applicability is limited, these correlations provide a reasonable estimate and more importantly allow for the calculation of temperature and species concentrations at the washcoat/channel flow interfaces. These wall conditions are then used in a porous catalytic washcoat sub-model with detailed surface chemistry to predict catalytic reaction rates in both the reforming and combustion channels.

2.2. Catalytic washcoat model

The catalytic washcoat layers for both the reforming and combustion channel flows are modeled as a finite volume (of a porous media) with a set of transient differential equations governing the gas-phase density and species mass fractions as well as the mole fractions on the catalyst surface and if the mechanism requires, in the bulk subsurface as well. The conditions in the washcoat were assumed to be uniform in the direction normal to the wall, even though it is understood that diffusion into the washcoat may impact the average gas-phase species and thus surface mole fractions (as characterized by a local catalyst effectiveness). However, a study of effectiveness vs. washcoat thickness indicated that catalyst effectiveness is reasonably approximated by a reduction in the catalyst area per unit washcoat volume. These issues related to washcoat catalyst effectiveness were not addressed in the current study, but have a minimal impact on the results and trends presented from the model.

While the conditions were assumed uniform in the direction perpendicular to the wall, washcoat conditions did vary in the axial direction, and the washcoats were discretized in correspondence with the gas-phase flow discretization in both channels. The governing equations for both the catalytic combustion and reforming washcoat layers are identical with only the chemistry mechanisms and the associated set of species being different. These governing equations are provided in alternative references [15,17] and are not presented here. In these equations, axial conduction of heat along the catalyst support due to solid-phase temperature gradients is included. Thus, the governing equations for temperatures in the washcoat and reactor substrate become second order PDE's due to the inclusion of axial conduction. These PDE's require two boundary conditions for the solid-phase temperatures at the entrance and exit of the respective channels. To this end, the boundary conditions are set based on an estimated conduction heat transfer to upstream flow at the front end of the reactor channel and an adiabatic condition for the downstream end of the channel.

2.3. Surface and gas-phase chemistry sub-models

The selection of catalyst/fuel combinations and appropriate surface chemistry mechanisms can have a tremendous impact on the model results, and thus the model was validated as described below with experimental measurements. For the catalytic combustion channel, a preliminary Pd–H_2–CH_4–O_2 surface chemistry mechanism [15,17] for supported polycrystalline Pd catalysts was employed. The catalytic combustion mechanism includes 35 elementary reaction steps for 10 surface species and two subsurface species PdO(bulk) and reduced Pd(bulk). This mechanism, which has undergone preliminary validation [15,17], has been shown to track well the hysteresis observed in PdO_x reduction/reoxidation cycles observed in TGA experiments [12,20] and as illustrated in Fig. 2, the mechanism predicts well the transition from ignition to mass transfer-limited conversion during catalyst light-off. Fig. 2 also shows the variation in axial profiles of CH_4 conversion—defined as $1 - Y_{CH_4}/Y_{CH_4,in}$, where Y_k is the local mass fraction of species k. The approach of conversion in washcoat to 1 signifies mass transfer limited combustion rates, where CH_4 is being oxidized as quickly as it is brought to the surface. The Pd–CH_4 combustion mechanism has not been shown to capture well re-ignition after the PdO_x catalyst loses its activity and thus further development on the mechanism is ongoing. Nonetheless, in its current form, the mechanism captures well the high temperature loss of activity at low O_2 partial pressures and thus is able to assess the stability of the Pd-based catalytic combustion process for the reforming reactions.

For CH_4 steam reforming over transition metal catalysts, detailed surface chemistry mechanisms remain largely uncertain although some mechanisms have been proposed for partial oxidation [16,21] of CH_4. The current study sought to adapt the recently presented CH_4 partial oxidation over Rh catalyst [16] for the current steam reforming study. It was found that as long as the steam to carbon ratio remained

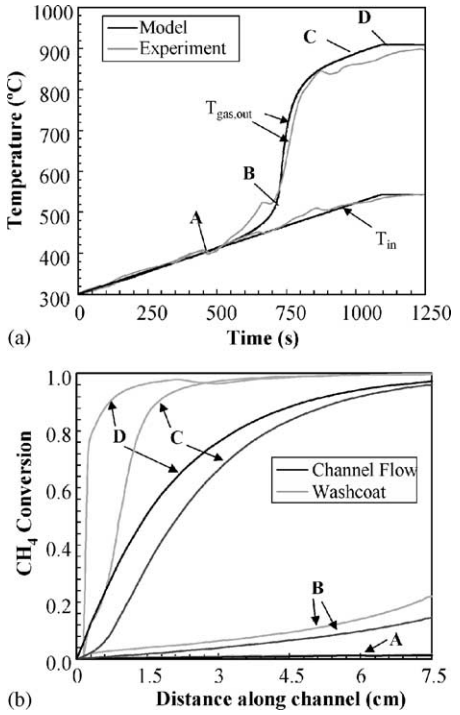

Fig. 2. (a) Comparison of experimental catalytic combustor exit temperatures with model results from single channel model for transient light-off of CH_4 over a washcoat-supported Pd catalyst. Conditions included constant inlet mass flux of 0.4 g/cm^2 s, fuel: CH_4 at $\phi_{comb} = 0.16$, and reactor length of 7.5 cm and channel diameter of 0.12 cm. (b) Profiles of CH_4 conversion for lettered points in (a) showing transition from light-off at B to mass transfer limited conversion at D.

adequately high, the partial oxidation mechanism did an adequate job of capturing the trends observed in steam reforming experiments.

For both the combustion and the reforming mechanism, the surface chemistry rate expressions were handled with necessary adaptations to Surface CHEMKIN [22] as discussed in the previous references. For the gas-phase chemistry, it was found that gas-phase reactions in the washcoat and the channel flow had a negligibly small contribution to CH_4 conversion for all conditions investigated in the current study. Thus, to increase the speed of the transient integration, gas-phase reactions were neglected and the gas-phase species were limited to the reactants and major products which desorbed from the catalyst (CH_4, CO_2, H_2O, O_2 and N_2 for the combustion mechanism and CH_4, CO_2, H_2O, CO, and H_2 for the reforming mechanism).

2.4. Numerical method

In the model, the spatially discretized governing equations for both channel flows and washcoat layers were combined into a single vector of differential algebraic equations and integrated simultaneously for both channel flows using the stiff ODE solver LIMEX [23]. Integration time steps were limited to 0.1 s. A discretization study indicated that cell lengths could be as large as 0.5 cm in the downstream region of the reactor without significantly impacting model results. On the other hand, near the reactor entrance (where heat and mass transfer coefficients vary significantly with distance due to entry effects), cell sizes were kept relatively small ($\leq$0.1 cm). For the 10 cm reactor channel length in the current study, a variable grid of 24 cells was sufficient for the model to capture the long-term transient results predicted by finer grids. A description of the catalyst/washcoat and the flow conditions used in the modeling results reported in this paper are given in detail in Table 1.

3. Experimental setup

To validate the model, experiments on a flat-plate reactor with simultaneous H_2 or CH_4 combustion and CH_4 steam reforming were conducted. A pre-oxidized Fecralloy substrate (1 mm thick) was coated on both sides with a γ-Al_2O_3 washcoat, which was approximately 20–40 μm thick after calcinations at 550 °C. The washcoat, which extended for 55 mm lengthwise along the Fecralloy plate, was then impregnated with Pd nitrate solution on the combustion side and Rh nitrate solution on the reforming side and calcined at 650 °C to form the Pd/γ-Al_2O_3 combustion catalyst and the Rh/γ-Al_2O_3 reforming catalyst. The Fecralloy plate was positioned in the reactor to create identical independent channels (20 mm across $\times$ 3 mm high in cross-section). The catalytic regions of the plate were placed downstream of premixing zones, which used loose quartz wool packing for enhanced mixing.

To reduce reactor heat losses, the reactor was maintained in a temperature programmable furnace at the defined reactant inlet temperature. The reactor flows were also preheated upstream of the furnace in order to minimize temperature non-uniformities upstream of the catalyst. Steam was introduced on the reforming

Table 1
Conditions for parallel plate reactor with integral catalytic combustion/steam reforming

	Catalytic combustion channel	Steam reforming channel
Catalyst/support	0.6% Pd on 50% porous Al_2O_3 washcoat on a Fecralloy support	1.7% Rh on 50% porous Al_2O_3 washcoat on a Fecralloy support
Surface chemistry mechanism	[17]	[16]
Catalyst area/washcoat volume	3000 cm^{-1}	6000 cm^{-1}
Channel length	100 mm	100 mm
Height (between plate centers)	3.2 mm	3.2 mm
Washcoat thickness	0.025 mm	0.025 mm
Inlet velocities	3.0 m/s, 6.0 m/s	$\leq$6.0 m/s
Inlet composition	H_2 or CH_4 ϕ_{comb}: 0.2, 0.3, 0.4	CH_4/H_2O: 0.5–1.1 (for experimental cases), CH_4/H_2O: 0.5–0.75 (otherwise)
Diluent	N_2	Ar (for experimental cases only)
Inlet conditions	T_{in} = 400–600 °C, P = 1, 4 bar	T_{in} = 400–600 °C, P = 1, 4 bar
Initial catalyst conditions	PdO_x (surface and in bulk phase)	Rh (surface and in bulk phase)

side by passing a diluent gas through a heated bubble saturator, and the saturator temperature controlled the steam mole fraction. Surface temperature measurements were made with (0.12 mm diameter) K-type thermocouples affixed to both sides of the substrate and positioned every 11 mm axially in the catalytic region as well as upstream of the catalytic region to assess heat conduction through the Fecralloy substrate.

Reforming effluent was measured by a VG Gaslab 300 quadrupole mass spectrometer in order to ascertain CH_4 conversion and H_2 selectivity. Argon was chosen as the diluent in the reforming flow to facilitate measurement of CO. The argon to steam ratio was maintained such that the moles of H_2 burned on the combustion side to moles of CH_4 reformed varied from 0.8 up to 6.0. These diluent ratios on the reforming side do not represent preferred reactor operating conditions for an actual application, but provide the necessary dilution of the steam for reliable exhaust gas analysis and thus model validation.

As the stable operating range for the reforming reactions over Rh exists between 600 and 900 °C, inlet temperatures below 600 °C required H_2 catalytic combustion to achieve rapid reactor light-off. This temperature window of high activity was captured surprising well by the surface chemistry mechanism and thus conversion in the reforming channels for both the experiment and the model was in large part a function of what portion of the reactor remained above 600 °C. The experimental tests for model validation used H_2 combustion over the supported Pd catalyst because heat losses in the experimental rig made for difficulties in maintaining stable performance with high reformate conversion and CH_4 as the combustion fuel. The conditions in the experimental study were designed to match closely those laid out for the numerical model in Table 1 with the exception that the experiments were performed exclusively at atmospheric pressure. It should be noted that these conditions were not chosen to achieve full conversion but rather to allow for intermediate conversions where the sensitivity of reactor performance to reactor flow rates is large. This facilitated model validation with the experiments.

4. Results

With the two independent flow streams, the integral catalytic combustor/steam reformer has several input parameters that can significantly impact catalyst temperatures and oxidation states and thus reactor performance. Due to the difficulties in testing numerous configurations, the current study was focused on development and validation of the catalyst surface chemistry models for a fixed geometry over a range of inlet conditions. The reactor model was used to study a broad range of reactor operating conditions. Maintaining steady-state performance in the experimental reactor with high reforming CH_4 conversion using CH_4 combustion as the heat source proved difficult in part due to heat losses at low temperature

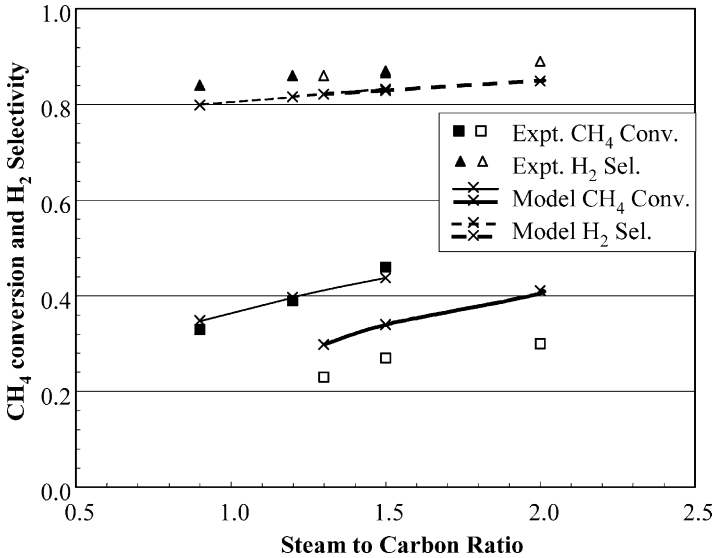

Fig. 3. Comparison of experimental results with numerical model predictions with H_2 combustion for reforming CH_4 conversion and H_2 selectivity. $T_{in} = 480\,^{\circ}C$, $\phi_{comb} = 0.4$, $v_{in,comb} = 5.1$ m/s and $v_{in,ref} = 0.9$ m/s. Thinner lines indicate model predictions where experimental temperature profiles are input to the model and the thicker lines indicate model predictions where temperature profiles are solved by the model.

and Pd catalyst deactivation at higher temperatures. Thus, the model was validated for reactor operation with H_2 combustion as the heat source, since H_2 combustion readily maintained high conversion in the reactor.

A comparison of model results with experimental measurements for both reforming CH_4 conversion and H_2 selectivity in the reformate exhaust are provided in Fig. 3. As can be seen in Fig. 3, for cases where the measured temperature profile was fixed in the model calculations, the model agreed well with experiments for both CH_4 conversion and H_2 selectivity for a range of steam to carbon ratios. For cases where the model was used to calculate temperature profiles, the model over-predicted CH_4 conversion and under-predicted H_2 selectivity, likely due to an under-assessment of heat losses in the model. The model was only compared with steady-state experimental results and not with the dynamic response because of the inability of the model to properly account for heat losses to the reactor housing, which slowed down the dynamic response of the experiments. All the same, the model does capture the transient development of the temperature profile along the length of the catalyst, including the initial peak early in the reactor and its transient decay to a steady-state value caused by reduction of the PdO_x combustion catalyst in the front end of the reactor. Agreement between experiments and the numerical models for conditions utilizing H_2 combustion suggests that the model is suitable for modeling trends in catalyst performance for a range of flow conditions. Further experimental testing for model validation has been undertaken for a broader range of conditions but is not reported here.

To assess the dynamic behavior of the combustion and reforming catalysts, the model was tested for a range of inlet conditions as indicated in Table 1. The range of reactor geometry and inlet conditions does not necessarily represent optimal configurations, but rather provides a basis for which to understand how parameters impact the performance of an integral catalytic combustion/steam reforming system using either H_2 or CH_4 as the combustion fuel and exclusively CH_4 as the reforming fuel. It is noted that due to the large heat sinks and heat sources in such close proximity, changes in catalyst loading and initial state can significantly influence whether the PdO_x combustion catalyst remains adequately oxidized for high activity. For the current study, the loadings were fixed and

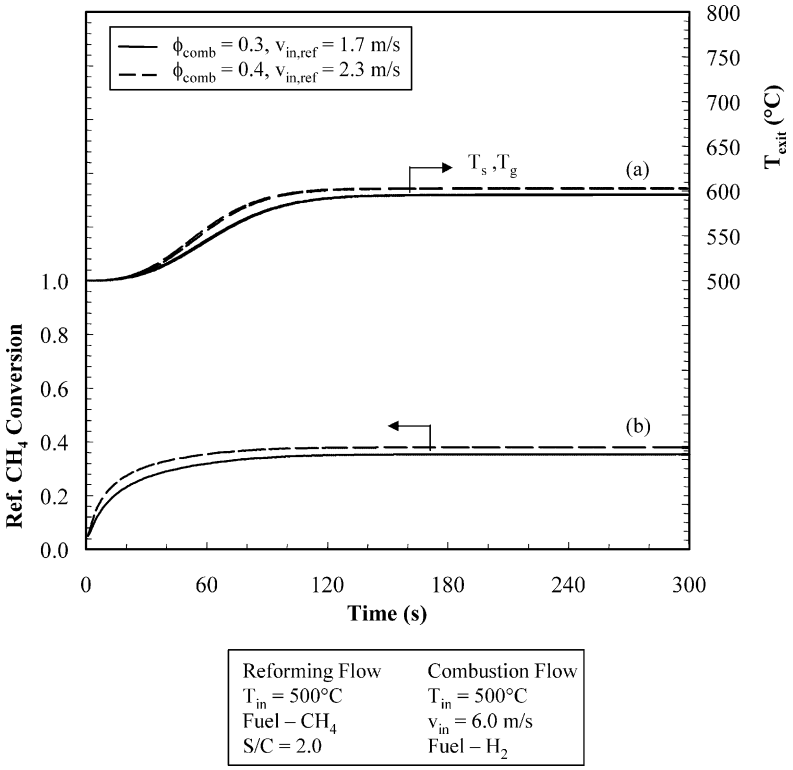

Fig. 4. Effect of ϕ_{comb} on transients in (a) exit gas phase in combustion channel and exit surface temperatures and on (b) CH_4 conversion in reforming channel for $T_{in} = 500\,^{\circ}C$. (Exit reforming gas phase temperatures are very close to surface temperatures.)

the combustion catalyst was initially specified as 99% oxidized on the surface and in the bulk of the catalyst particles.

For the subsequent model results, the diluent used in the experimental validation is removed from the reforming channel flow, and $v_{in,ref}$ is set to one of three conditions: (1) reforming fuel flow is equal to the autothermal flow rate, (2) reforming fuel flow is approximately twice that of the autothermal flow rate, and (3) reforming fuel flow is approximately half that of the autothermal flow rate. Autothermal operation is defined as conditions where the heat uptake for complete conversion of the reforming flow equals the heat release for complete combustion in the combustion channel. For lower inlet temperatures ($\leq$500 °C), stable catalyst operation with high reformate conversion requires reforming flow rates to be less than autothermal rates in order to ensure adequate temperature rise in the reactor.

Model runs were performed by transient integration for 20 min. Fig. 4 shows the transient catalyst ignition indicated by exit temperatures (both on the surface and in the gas phase) and by reforming fuel conversion for near autothermal cases with an inlet temperature of 500 °C. The H_2 conversion on the combustion side rises to >0.99 in the first 3 s for both cases and thus is not shown in Fig. 4. Fig. 4 indicates that by keeping the combustion fuel to reforming fuel ratio constant through adjusting $v_{in,ref}$, reactor performance does not strongly depend on ϕ_{comb} for such conditions with H_2 combustion. A plot of the spatial profiles at $t = 60$ s in Fig. 5a of surface temperature and combustion gas flow temperature for these cases indicates the slight differences in catalyst behavior due to ϕ_{comb}. In Fig. 5a, it can be seen that the combustion conversion occurs very rapidly at the reactor front end due to the narrow passageways (0.159 cm) and high mass transfer rates to the catalyst near the reactor leading edge.

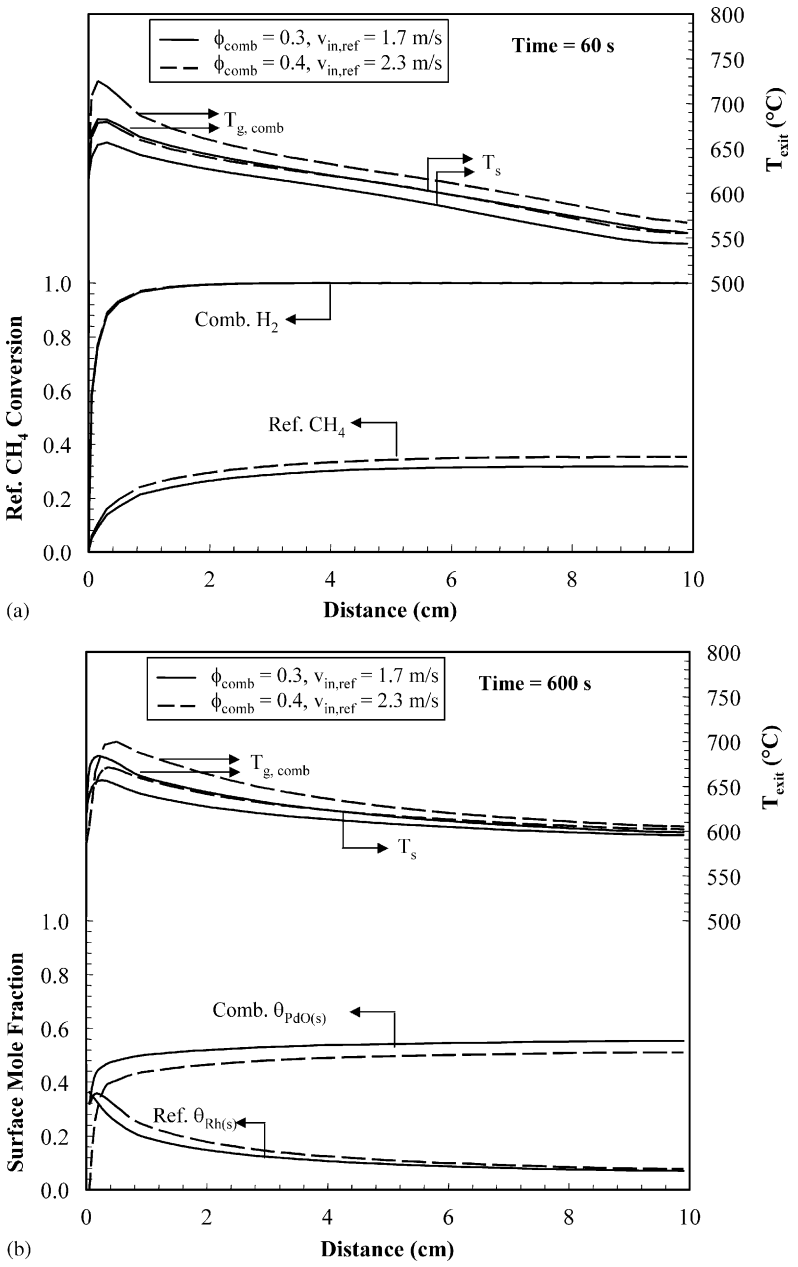

Fig. 5. (a) Profiles of temperature and conversion of fuel in both channels at $t = 60$ s for $\phi_{comb} = 0.3$ and 0.4 at $T_{in} = 500\,^{\circ}C$. (b) Near steady-state profiles at $t = 600$ s of critical surface site fractions and temperature along the reactor length for same conditions as in (a).

The higher ϕ_{comb} (=0.4) initially causes a more rapid temperature rise and increases the rate of steam reforming on the Rh catalyst, which results in a slightly higher CH_4 conversion to H_2.

For the reforming mechanism, the key reaction to which CH_4 conversion is highly sensitive is the two-step dissociative adsorption of CH_4 on vacant Rh(s) sites as indicated by reactions (2) and (3):

$$CH_4 + Rh(s) \rightarrow Rh\text{–}CH_4(s) \quad (2)$$

$$Rh\text{–}CH_4(s) + Rh(s) \rightarrow Rh\text{–}CH_3(s) + Rh\text{–}H(s) \quad (3)$$

Thus, a reforming Rh catalyst is most effective when it maintains a high site fraction of Rh(s), i.e. $\theta_{Rh(s)}$. Fig. 5b shows that the near steady-state profiles of $\theta_{Rh(s)}$ for the two different ϕ_{comb} differ substantially only in the first few millimeters near the front end of the reactor. The shapes of the $\theta_{Rh(s)}$ largely follow those of the surface temperature profiles, and reactor surface temperature appears to be the critical factor in determining the effectiveness of the Rh catalyst.

For combustion conversion, the controlling reaction according to the surface chemistry mechanism [17] for both H_2 and CH_4 is largely dissociative adsorption of the fuel molecule on an oxide/vacancy (PdO(s)/Pd(s)) pair site. This reaction indicated for each fuel in reactions (4) and (5) is more dominant in CH_4 combustion over the Pd catalyst and this is discussed further below:

$$H_2 + Pd(s) + PdO(s) \rightarrow PdO\text{–}H(s) + Pd\text{–}H(s) \quad (4)$$

$$CH_4 + Pd(s) + PdO(s) \rightarrow PdO\text{–}H(s) + Pd\text{–}CH_3(s) \quad (5)$$

If the temperatures in the combustion catalyst rise too rapidly, combustion fuel conversion in the catalyst can drop due to a loss in $\theta_{PdO(s)}$. This behavior is more critical for CH_4 combustion since the dissociative adsorption of H_2 on reduced Pd(s) also occurs relatively fast [24], whereas CH_4 dissociative adsorption on reduced Pd(s) has a substantially higher activation energy than reaction (5) [16]. As seen in the steady-state profiles of $\theta_{PdO(s)}$ for the two autothermal cases with H_2 combustion, only for ≈0.2 cm near the front end of the reactor at the higher ϕ_{comb} does the Pd catalyst undergo significant loss of surface oxide. This results in a loss in combustion activity and a slower rise in

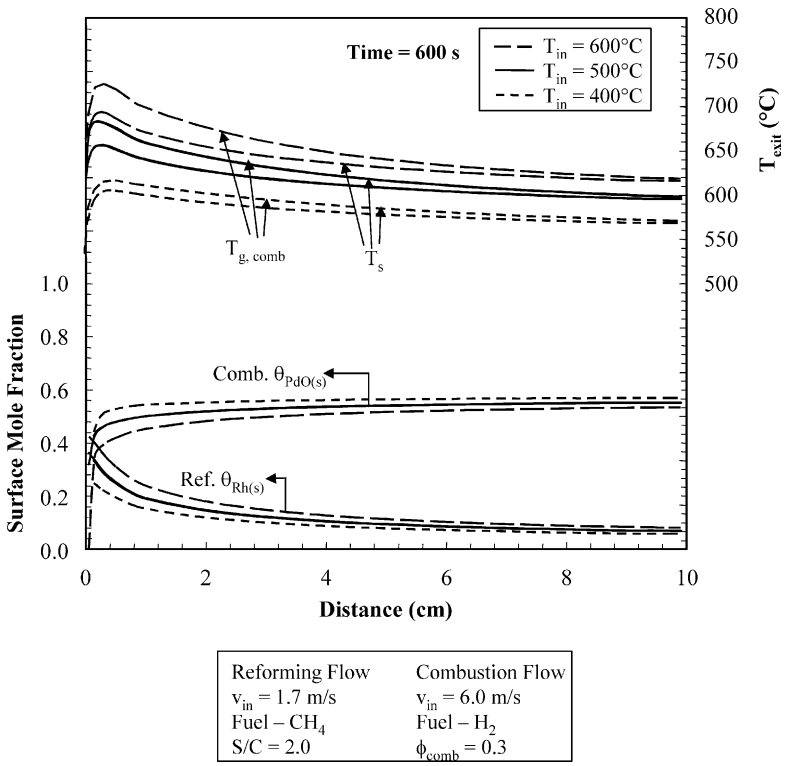

Reforming Flow	Combustion Flow
v_{in} = 1.7 m/s	v_{in} = 6.0 m/s
Fuel – CH_4	Fuel – H_2
S/C = 2.0	ϕ_{comb} = 0.3

Fig. 6. Effect of T_{in} on steady-state profiles of critical surface site fractions in both channels and on reactor temperature profiles for $\phi_{comb} = 0.3$.

temperatures at the front end of the reactor. This reduction at the front end of the combustion catalyst does not occur after 60 s (as indicated in Fig. 4), but has reached near its steady-state value at 600 s, thus indicating the slow transients in PdO_x oxidation states. With the backside integral reactor however, the endothermic reforming mitigates the catalyst temperature rise and actually prevents the catalyst from reaching temperatures which result in PdO(s) reduction further downstream in the reactor. This maintains reforming fuel conversion downstream in the reactor. Steady-state values of CH_4 conversion in the reforming stream for the two cases in Figs. 4 and 5 are very similar −0.35 for $\phi_{comb} = 0.3$ and 0.37 for $\phi_{comb} = 0.4$.

With H_2 as the combustion fuel, both experiments and modeling results indicate that reforming CH_4 conversion can be sustained for near autothermal conditions with H_2 combustion ($\phi_{comb} = 0.3$) for T_{in} as low as 400 °C. Fig. 6 shows how T_{in} influences predicted reactor temperatures and Rh and PdO_x catalyst surface site fractions for these near autothermal conditions. Since reforming rates on the Rh catalyst are quite slow below 600 °C, the surface and combustion gas-phase temperatures rise more significantly for the $T_{in} = 400$ °C. However, this increased temperature rise still does not provide adequately high surface temperatures for sustained reforming, whereas the higher T_{in} cases, which provide the entire length of the reactor with $T_s > 600$ °C, do result in substantially higher reforming fuel conversion rates. Steady reforming CH_4 conversion for these model runs are 0.20, 0.35, and 0.52 for $T_{in} = 400$, 500, and 600 °C, respectively. The surface site fractions associated with these three cases are also shown in Fig. 6. Although the case with $T_{in} = 400$ °C has the highest PdO(s) site fraction on the combustion catalyst, the lower temperatures result in the build-up of Rh–CO(s) which limits activity for reactions (2) and (3) and prevents high CH_4 conversion. The $\theta_{PdO(s)}$ curves in Fig. 6 indicate that for the lower ϕ_{comb} even at the highest inlet temperature, very

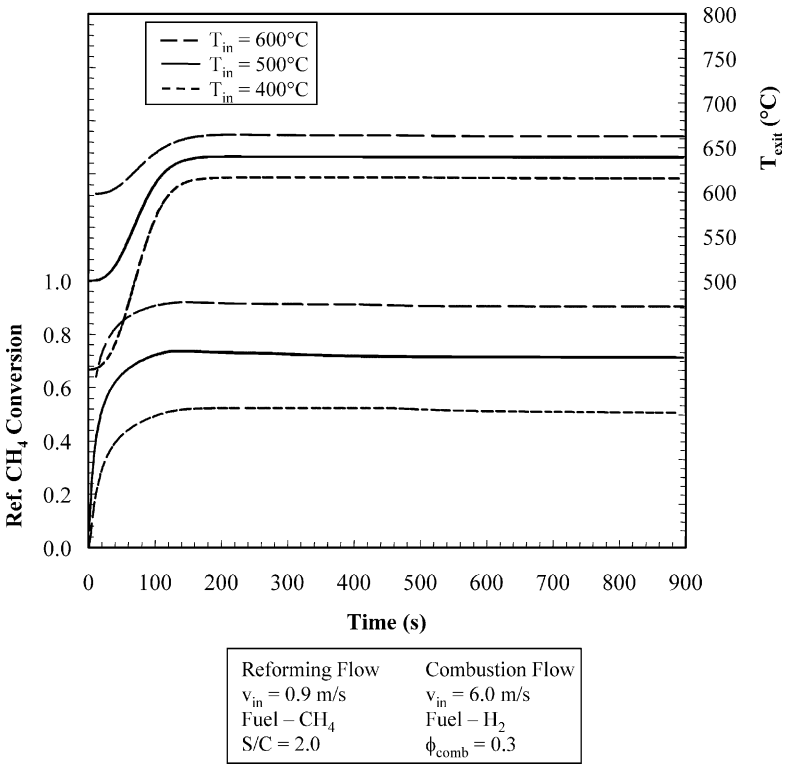

Fig. 7. Transient profiles of conversion in reforming channel and exit temperatures for a range of T_{in} with excess combustion showing slight decay in conversion with time due to combustion catalyst reduction.

little of the PdO_x catalyst has undergone complete reduction and thus high combustion catalyst activity is maintained because of the mitigating effects of the reforming reactions and the convective heat transfer to the backside reforming flow. It should be noted that for all three of these cases, models of adiabatic combustion without the backside steam reforming would cause PdO_x reduction across a large fraction of the length of the catalytic surface.

The effects of T_{in} are somewhat altered when the combustion fuel flows are increased to exceed autothermal flow rates. Under these conditions, the rise in temperature even for $T_{in} = 400\,^{\circ}C$ is adequate to provide reactor surface temperatures high enough for substantial CH_4 conversion over the Rh catalyst. This is shown in the transient temperature profiles in Fig. 7 and also in the CH_4 conversion (=0.50 at steady state) for $T_{in} = 400\,^{\circ}C$. Reforming CH_4 driven by H_2 catalytic combustion with $T_{in} = 400\,^{\circ}C$ was also observed in the experiments. For the higher temperatures, the front end of the reactor does experience a reduction in the PdO_x combustion catalyst which results in a transient decay in the reactor temperature rise at the front end as indicated for $T_{in} = 500\,^{\circ}C$ by comparing Fig. 5a and b. However, the Rh catalyst provides adequate reforming activity and thus cooling of the combustion catalyst such that $\theta_{PdO(s)}$ remains >0.3. The ability for the reactor to sustain such high reforming activity to cool the combustion catalyst is assisted by the fact that the reforming catalyst is twice as heavily loaded as the combustion catalyst (Table 1). Fig. 7 shows a slight decay in reforming conversion with time even out to 900 s for the higher T_{in} cases. This decay arises from the slow reduction of the PdO_x catalyst near the front end of the integral reactor.

Since the combustion surface chemistry mechanism is designed for CH_4 combustion on PdO_x, numerous simulations were run with CH_4 as the combustion

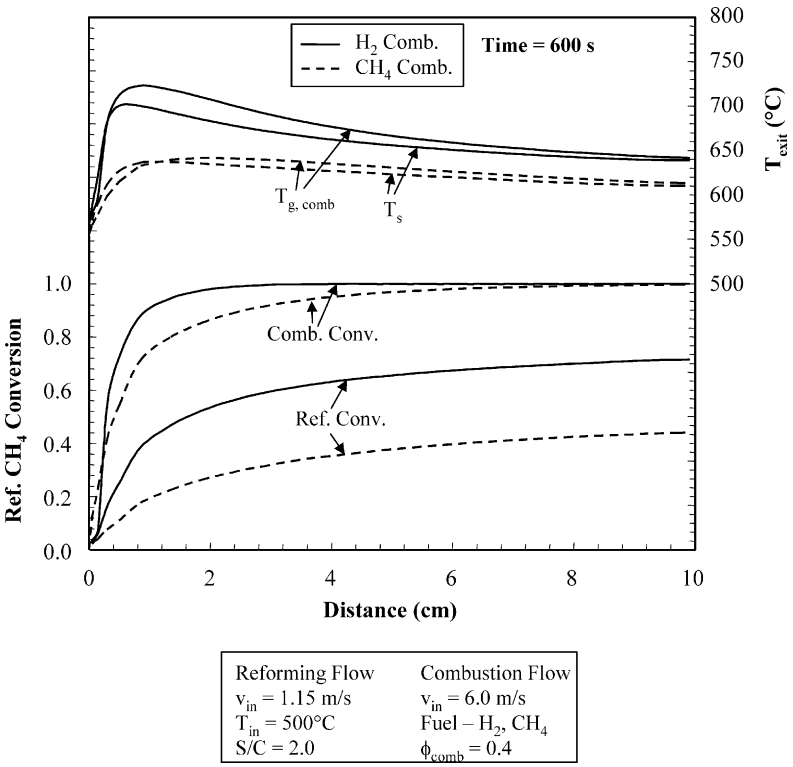

Fig. 8. Effect of combustion fuel source on steady-state profiles of conversion in both channels and temperature at $\phi_{comb} = 0.4$ and $T_{in} = 500\,^{\circ}C$.

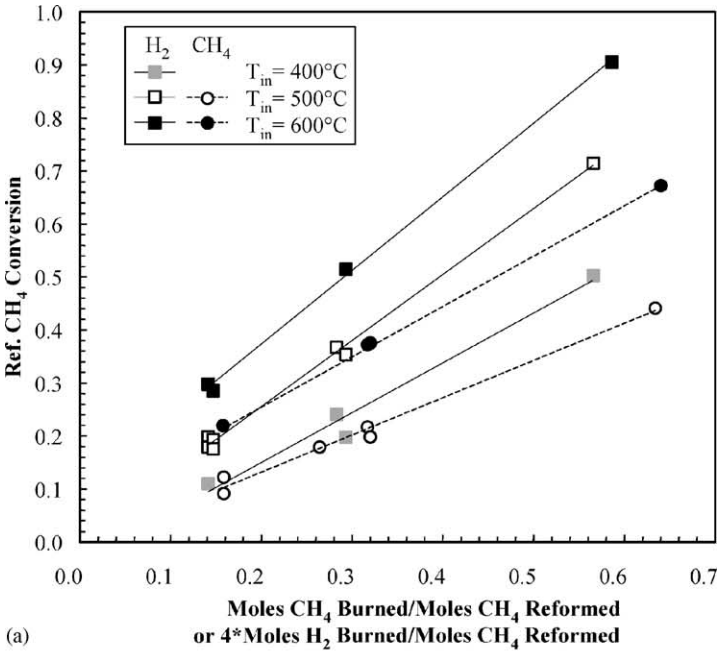

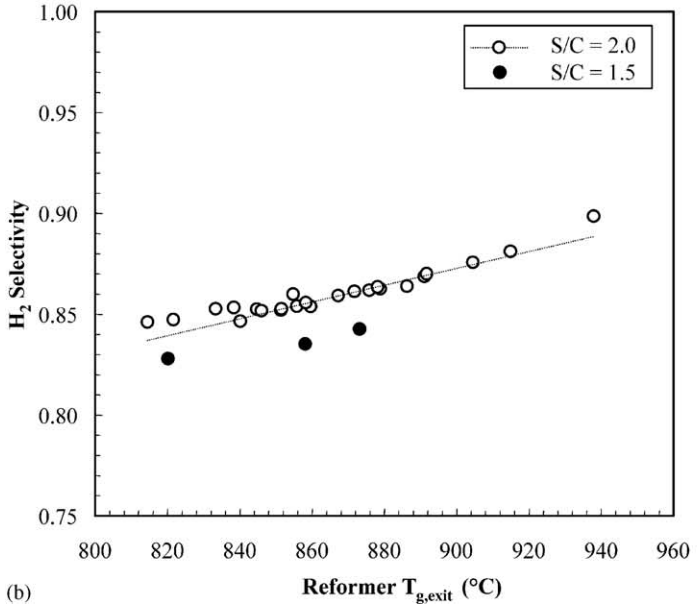

Fig. 9. (a) Plot showing reforming CH_4 conversion as a function of the ratio of moles of fuel to combustor to the moles of fuel to the reformer for a range of T_{in}. (b) Plot of H_2 selectivity in reformer exhaust as a function of reformer exit temperature.

fuel. Although Pd/PdO_x is considered the most active catalyst for CH_4 combustion, the combustion rates are substantially slower than H_2 combustion on the same catalyst. The slower reactions rates prohibit CH_4 catalytic combustion from providing adequate heat release at 400 °C to sustain reforming reactions. At the higher inlet temperatures, CH_4 catalytic combustion is more susceptible to deactivation from catalyst

reduction but can be sustained even under the non-adiabatic conditions caused by backside reforming. A comparison is shown in Fig. 8 of model results with H_2 combustion and CH_4 combustion for $T_{in} = 500\,^{\circ}C$ and $\phi_{comb} = 0.4$ and with reforming flow rates less than autothermal values. Under these conditions, the H_2 combustion results in PdO_x reduction at the reactor front end, which causes the initial slow rise in combustion conversion. However, the sub-unity Lewis number of H_2 causes a rapid rise in surface temperature in spite of the slower conversion rates, and this rapid temperature rise has been reported in other studies of H_2 oxidation [25]. The rapid temperature rise for the H_2 combustion allows for faster reforming rates which are then sustained further downstream because of the higher adiabatic temperature (i.e. heat release) for the same ϕ in comparison to CH_4.

From numerous runs with CH_4 or H_2 as combustion fuel, both steady-state conversion and H_2 selectivity have been assessed. The results for CH_4 conversion in the reforming flow for these cases are plotted against the ratio of moles of fuel into the combustor to moles of fuel into the reformer in Fig. 9a. To plot H_2 on the same scale as CH_4, H_2 molar flow rates into the combustor were divided by 4.0 to put the fuels on the same basis with respect to O_2 consumption rates. The results plotted in Fig. 9a show some scatter due to differences in ϕ_{comb}, $v_{in,comb}$, and other variables that have a secondary effect on reforming fuel conversion in comparison to the primary effects of ratio of combustion to reforming fuel flows and T_{in}. The results in Fig. 9a show an unexpected linear increase in conversion with respect to the ratios of fuel flows. The H_2 combustion cases show a more rapid increase with the ratio of fuel flows than the CH_4 combustion cases, and this may be in part be attributed to the rapid temperature rise at the front end of the catalyst due to the sub-unity Lewis number.

Fig. 9b plots H_2 selectivity as a function of reformer exit temperature for a range of conditions.

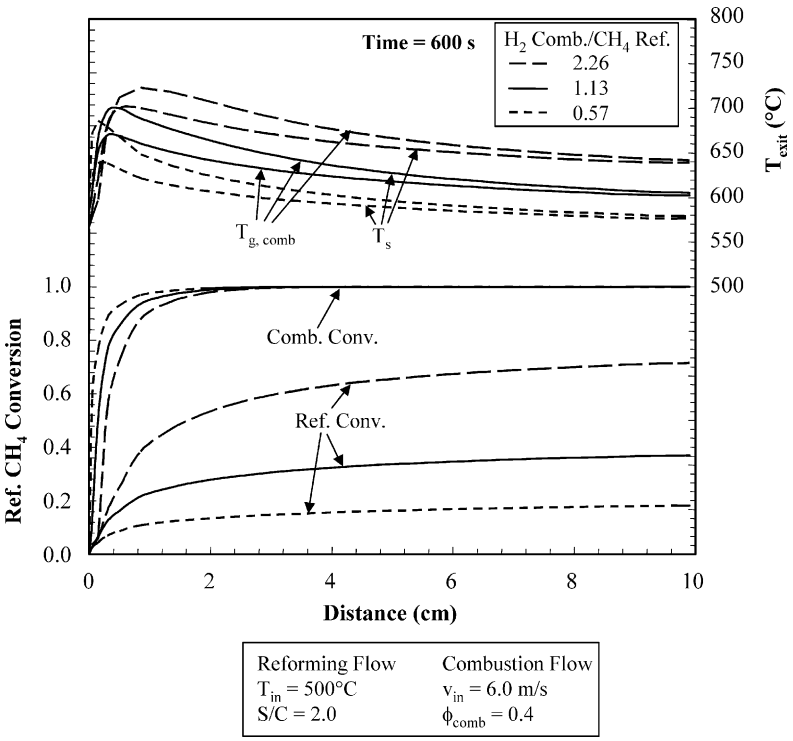

Fig. 10. Effect of the ratio of moles fuel into combustor to moles fuel into reformer on steady-state CH_4 conversion in the reforming channel and on reactor temperature profiles for $\phi_{comb} = 0.4$ and $T_{in} = 500\,^{\circ}C$.

The reformer exit temperature, which closely matches the exit surface temperature for the conditions in this study, plays a dominant role in determining H_2 selectivity for a fixed steam to carbon ratio in the reformer. The plot in Fig. 9b suggests that the Rh catalyst is effective at driving the reformate composition toward an equilibrium. However, the positive slope of the curve in Fig. 9b suggests that equilibrium in the gas phase has not been obtained. The open symbols, which indicate a steam to carbon ratio of 2.0, include a wide range of conditions based on inlet velocities, ϕ_{comb}, and T_{in}. Cases with a lower steam to carbon ratio (=1.5) show a significant drop in H_2 selectivity as expected.

In light of the results in Fig. 9a showing the importance of the ratio of combustion fuel flows to reforming fuel flows, a plot of the temperature and conversion profiles for three different ratios of combustion fuel to reforming fuel are shown in Fig. 10. These cases correspond to a reforming flow rate approximately twice the autothermal rate, nearly equal to the autothermal rate, and approximately half of the autothermal rate. Although the combustion conversion for each case is >0.99. The reforming CH_4 conversion increases with decreasing flow rate, conversion = 0.18, 0.37, and 0.71, respectively, as reforming flow rate decreases. It should be noted that the autothermal case provides the highest rate of H_2 production as determined by multiplying the conversion by the reformer flow-rate. This fact attests to the importance of maintaining both the combustion catalyst and the reforming catalyst at their optimal operating conditions (with high $\theta_{PdO(s)}$ and $\theta_{RH(s)}$ site fractions, respectively). The reformer flow rates below autothermal rates result in initially high temperatures at the front end of the reactor which result in PdO(s) reduction and a subsequent decay in combustion conversion and surface temperature at the front end of the reactor. The resulting loss in activity is not recovered upon cooling for the conditions in Fig. 10 due to the hysteresis in the PdO oxidation and reduction [12,26]. This results in a reduction in the effectiveness of the upstream region of the reactor for providing heat for the endothermic reforming and more of the conversion is shifted downstream. The results in Fig. 10 also indicate the importance of using complex chemistry mechanisms to model catalytic reactor performance. The ability to capture the PdO(s) reduction is critical for predicting the complex trends in the reactor performance.

5. Conclusions

The integration of catalytic combustion with steam reforming in a co-flow heat exchanger has been investigated through the use of a transient reactor model with detailed surface chemistry mechanisms for both processes. The results along with validation experimental studies revealed the importance of implementing a high activity reforming catalyst, in this case supported Rh, to provide adequate heat removal for the combustion catalyst to operate without excessive dilution of the combustion fuel. Both H_2 and CH_4 combustion were studied as heat sources for the reforming reaction and the model predicted higher reforming conversion rates with H_2 as the combustion fuel due to the more rapid temperature rise at the front end of the reactor and the ability of the H_2 to continue oxidation (albeit at slower rates) when the PdO_x combustion catalyst undergoes reduction. Because the model implements a mechanism for Pd–CH_4 catalytic combustion that can capture catalyst reduction and subsequent loss of activity, interesting trends emerge from the parametric study including an optimal ratio of combustion fuel flow rates to reforming fuel flow rates as a function of T_{in}. For $T_{in} = 500\,^{\circ}C$, autothermal ratios of fuel flows appears to provide the highest molar rate of H_2 production per mole of fuel burned.

The results in this study, which are derived from the coupling of two complex catalytic chemistries, indicate the value in continuing to pursue catalyst surface chemistry models, and in particular, for combustion on Pd-based catalysts and for catalytic steam reforming. Such mechanisms will assist in the development of more reliable models for the design and optimization of complex catalytic systems as discussed in this study. Such efforts can provide valuable understanding for developing new volumetrically efficient reactor designs for H_2 production using integral catalytic combustion/steam reforming.

Acknowledgements

The authors acknowledge the support of the California Energy Commission (Hal Clark, Program Manager) under EISG Grant #99-21 and of NSF (Dr. Farley Fisher, Program Manager) under Grant No. CTS-9984293.

References

[1] A.L. Dicks, J. Power Sources 61 (1996) 113.
[2] D.L. Trimm, Z.I. Onsan, Catal. Rev. 43 (2001) 31.
[3] F. Joensen, J.R. Rostrup-Nielsen, J. Power Sources 105 (2002) 195.
[4] S.T. Adelman, M.A. Hoffman, J.W. Baughn, J. Eng. Gas Turb. Power 117 (1995) 16.
[5] J.N. Phillips, R.J. Roby, Power Eng. 104 (2000) 36.
[6] G.L. Ohl, J.L. Stein, G.E. Smith, J. Energy Res. Technol. 118 (1996) 112.
[7] E.A. Polman, J.M. Der Kinderen, F.M.A. Thuis, Catal. Today 47 (1999) 347.
[8] Z.R. Ismagilov, V.V. Pushkarev, O.Yu. Podyacheva, N.A. Koyabkina, H. Veringa, Chem. Eng. J. 82 (2001) 355.
[9] S. Freni, G. Calogero, S. Cavallaro, J. Power Sources 87 (2000) 28.
[10] J.G. McCarty, Y. Chang, Scripta Metall. Mater. 31 (1994) 1115.
[11] M. Lyubovsky, L.D. Pfefferle, Appl. Catal. A 198 (1998) 107.
[12] R.J. Farrauto, M.C. Hobson, T. Kennelly, E.M. Waterman, Appl. Catal. A 81 (1992) 227.
[13] J.R. Rostrup-Nielsen, in: J.R. Anderson, M. Boudart (Eds.), Catalysis: Science and Technology, vol. 5, Springer, New York, 1984.
[14] E.C. Luna, A.M. Becerra, M.I. Dimitrijewits, React. Kinet. Catal. Lett. 67 (1999) 247.
[15] H. Zhu, Ph.D. Dissertation, University of Maryland, College Park, MD, 2001.
[16] O. Deutschmann, R. Schwiedernoch, L.I. Maier, D. Chatterjee, in: E. Iglesia, J.J. Spivey, T.H. Fleisch (Eds.), Natural Gas Conversion VI, Studies in Surface Science and Catalysis, vol. 136, Elsevier, Amsterdam, 2001, pp. 215–258.
[17] H. Zhu, G.S. Jackson, ASME Paper No. 2001-GT-0520, ASME, New York, 2001.
[18] G.A. Groppi, A. Belloli, E. Tronconi, P. Forzatti, Chem. Eng. Sci. 50 (1995) 2705.
[19] G.A. Groppi, W. Ibashi, M. Valentini, P. Forzatti, Chem. Eng. Sci. 56 (2001) 831.
[20] A.B. Datye, J. Bravo, T.R. Nelson, P. Atanasova, M. Lyubovsky, L.D. Pfefferle, Appl. Catal. A 198 (2000) 179.
[21] D.A. Hickman, L.D. Schmidt, Science 259 (1993) 343.
[22] M.E. Coltrin, R.J. Kee, F.M. Rupley, E. Meeks, SURFACE CHEMKIN-III: a FORTRAN package for analyzing heterogeneous chemical kinetics at a solid-surface gas-phase interface, Sandia National Lab Report SAND96-8217, 1996.
[23] P. Deuflhard, E. Hairer, J. Zugck, Numer. Math. 51 (1987) 501–516.
[24] D. Söderberg, I. Lundström, Solid State Commun. 45 (5) (1983) 431.
[25] L.L. Hegedus, AIChE J. 21 (1975) 849.
[26] A.K. Datye, J. Bravo, T.R. Nelson, P. Atanasova, M. Lyubovsky, L. Pfefferle, Appl. Catal. A 198 (2000) 179.